

# HT-search for alkaline- and noble-metal-free mixed oxide catalysts for soot oxidation

Nelson E. Olong, Klaus Stöwe, Wilhelm F. Maier\*

*Lehrstuhl für Technische Chemie, Universität des Saarlandes, 66123 Saarbrücken, Germany*

Available online 18 April 2008

## Abstract

High-throughput techniques have been applied to search for soot oxidation catalysts free of noble metals and alkaline metals. Libraries consisting of up to 206 catalysts were screened for relative heats of reaction by emissivity-corrected infrared thermography. Using this approach, new catalyst formulations capable of combusting soot at relatively low temperatures were discovered. The hits identified via the high-throughput experimentation were successfully synthesized and tested conventionally using thermogravimetric analysis. The highest activity of the  $\text{Pb}_{10}\text{La}_5\text{Co}_{85}\text{O}_x$  catalyst was found to be maintained after calcination at 700 °C. A good correlation between XRD and transmission electron microscope (TEM) measurements was achieved. Electron dispersive X-ray (EDX) analysis at specific points revealed a homogeneous distribution of the various constituents of the catalysts as expected based on the sol–gel method used.

© 2008 Elsevier B.V. All rights reserved.

**Keywords:** Combinatorial method; Soot; Mixed metal oxides; Sol–gel

## 1. Introduction

Diesel engine emission of particulate matter (PM) and nitrous oxides ( $\text{NO}_x$ ) is of increasing concern with regard to human health and the environment. The EU Commission and the Environmental Protection Agency (EPA) in the US are highlighting *fine particulate* as one of the current priorities for environmental hygiene. Presently most of the world's auto-makers are concentrating on developing and using diesel particulate filter to trap soot from the exhaust gas [1]. While trapping has been solved, the filter regeneration (soot combustion) is subject of concern and present solutions are not optimal. The commercialized diesel particulate matter filter (DPF) regeneration technologies are either additive based, catalysed filter-based or continuous regenerating filter-based (CRT) [2]. Although research has been intensified, especially the catalysts developed for DPF do not meet expectation. Especially the noble metal contents and the relatively high operating temperatures of state of the art materials are undesired, an acceptable catalyst that will meet future legislative limits has not yet been discovered. Among the

transition metals, cobalt oxide, molybdenum oxide, lead oxide and mixtures of them have been proposed early on for soot combustion under tight contact between soot and catalyst [3,4]. Thermogravimetric analysis has become most common to determine the effect of catalysts on soot oxidation [4,5]. However, the major problem of soot combustion is its fundamental particulate nature, which does not allow tight contact between soot and catalyst particles. Therefore soot oxidation is significantly different from classic oxidation catalysis, in which molecular chemisorption on an active center precedes the catalytic oxidation step. In soot oxidation, activated oxygen species must somehow diffuse from the center of oxygen activation to the soot particle to cause combustion. Therefore, only a loose contact between soot and catalyst can model realistically conditions in a diesel particulate filter [5]. It is well known, that the mixing of the soot with the catalyst affects performance. The more pressure is applied to form the mixture, the lower is the temperature of combustion [4,6]. Because of these problems with diesel soot oxidation, catalysts are often developed by tedious one at a time methods with subsequent activity testing and characterization. Although these methods have led to the discovery of several promising catalysts, a large unexplored universe of materials remains that may pose superior catalytic activities.

\* Corresponding author. Tel.: +49 681 302 2582; fax: +49 681 302 2343.

E-mail address: [w.f.maier@mx.uni-saarland.de](mailto:w.f.maier@mx.uni-saarland.de) (W.F. Maier).

High-throughput techniques have also been applied to the discovery of new catalyst formulations [7–10]. Combinatorial methods and high-throughput experimentation allow the synthesis and screening of a large number of catalysts within short time periods. In our group both sequential and parallel screening techniques have been used to search for new or optimized heterogeneous catalysts [11–13]. For soot combustion, which is an exothermic reaction, a parallel screening technique is the most appropriate method. Since the whole catalyst–soot library is maintained at the same temperature, the soot of all the catalyst–soot spots will be oxidized simultaneously. Therefore sequential operation cannot be applied here and parallel detection is required. The use of sequential techniques would require to heat the catalyst–soot spots sequentially. McGinn and coworkers used automated thermogravimetric analysis to study the effect of alkali metal-doped oxides for diesel soot combustion. The authors came to a conclusion that this approach was slow, with characterization of individual compositions requiring approximately 75 min each [14]. In a previous study [15], we have successfully applied emissivity-corrected IR-thermography for the parallel screening of libraries with up to 206 catalyst–soot mixtures. The hits from screening have been validated by conventional thermogravimetric analysis (TGA). The most active catalysts discovered also contained alkaline ions, confirming the trends reported in [14]. Alkali metal ions have been reported already in earlier studies to improve the catalyst activity and mobility, which may result in an intimate contact between soot and catalyst. But on the other hand increased mobility may also lead to catalyst degradation [16]. A well-known problem for alkali dopants is the leaching of the alkali ions in the presence of water vapor. Therefore in this contribution alkaline- and noble-metal-free soot oxidation catalysts have been searched for by high-throughput experimentation. ec-IRT has been used for primary screening and TGA was applied for validation of hits. For catalyst preparation (mixed oxides), sol–gel procedures tolerant to compositional changes [17] have been chosen.

## 2. Experimentation

### 2.1. High-throughput catalyst preparation

In high-throughput searches for new catalyst compositions it is essential, that catalysts preparation is carried out under identical conditions. Variation in chemical composition or doping with a wide range of elements must be carried out with a common synthesis procedure that is very tolerant to such compositional changes. The sol–gel method, whose validity to synthesize catalyst materials has been proven before, was deployed for the syntheses of the mixed metal oxides considered in this work [12,18]. The sol–gel recipes used allow broad screening of elemental compositions. Furthermore this method allows the preparation of metal oxides in the liquid phase at room temperature and atmospheric pressure. These properties facilitate the coupling of the sol–gel method to a synthesis robot, thereby increasing the speed at which materials are synthesized. The design of the material libraries was

accomplished with help of the software “Plattenbau” [19]. This software calculates on the basis of a parameterized recipe the volumes of the different solutions of starting materials, as required for the preparation of the individual samples and generates an optimized pipetting list, which was transferred directly to a pipetting robot (Lissy, Zinsser Analytic). A 1-M solution of the basic metal ion (here mostly Co-propionate in methanol) in the form of a precursor solution was positioned in a 20-ml vial. A 0.1-M solution of 50 different elements in the form of nitrates (Ag, Al, Ba, Ca, Cd, Ce, Cr, Cu, Dy, Er, Eu, Fe, Ga, Gd, Ho, In, La, Lu, Mg, Mn, Na, Nd, Ni, Pr, Sc, Sm, Sr, Tb, Tm, Y, Yb, and Zn), alkoxides (Ta, Ge, Mo, Bi, Sn, Si, Ti, V, and Zr), acetate (Pb), chlorides (Hf, W, Te, Sb, Sn, and Ru), bromide (Pt), hydroxide (B) or oxide (Se) dissolved in methanol were each placed in a 10-ml vial. The final reaction mixtures were prepared by pipetting the appropriate volumes of dopants and matrix material in 2 ml GC vials, which were positioned in a rack of 50 vials. The preparation of  $\text{Ce}_3\text{Co}_{97}$  for example was performed by pipetting the following volumes of single solutions in sequence: methanol (226.6  $\mu\text{l}$ , 5.6 mmol), 4-hydroxy-4-methyl-2-pentanone (112  $\mu\text{l}$ , 900  $\mu\text{mol}$ ), cobalt propionate (291  $\mu\text{l}$ , 291  $\mu\text{mol}$ ), and cerium nitrate (90  $\mu\text{l}$ , 9  $\mu\text{mol}$ ) in a 2-ml vial. After the pipetting process of the entire rack was completed, the rack was agitated on an orbital shaker (Heidolph, Titramax 100) for 1 h and dried for 5 days at room temperature. For calcination the samples were placed in an oven, heated to 400 °C at a heating rate of 1 °C/min under static air and kept there for 5 h.

The same recipe was used to synthesize ternary (cerium, cobalt, and molybdenum) and pentanary (cerium, cobalt, molybdenum, lanthanum and vanadium) composition spread samples. The preparation of  $\text{Co}_{20}\text{Mo}_{40}\text{Ce}_{40}$  for example was as follows: 60  $\mu\text{l}$  (60  $\mu\text{mol}$ ) of a 1-M solution of cobalt nitrate in methanol, 120  $\mu\text{l}$  (120  $\mu\text{mol}$ ) of a 1-M solution of molybdenum isopropoxide in isopropanol and 120  $\mu\text{l}$  (120  $\mu\text{mol}$ ) of a 1-M solution of cerium nitrate in methanol were pipetted into a 2-ml vial. Finally 112.5  $\mu\text{l}$  (900  $\mu\text{mol}$ ) of an 8-M mixture of 4-hydroxyl-4-methyl-2-pentanone as complexing agent and propionic acid solution was added. The resulting mixture was stirred for 1 h and then dried at 40 °C for 5 days to allow gel formation and catalyst drying. Successively, the samples were calcined in an oven at 400 °C, using a heating rate of 0.2 °C/min and kept at this temperature for 5 h under static atmosphere. The central elements with the atomic% given in subscripts as expected from the composition of the starting sol are used to denote the samples. For example  $\text{Ce}_3\text{Co}_{97}$  is a mixed metal oxide composed of 3 mol% Ce oxide and 97 mol% Co oxide. The oxidation states of the mixed oxides, which rely on the reaction conditions, were not determined. Therefore the oxygen content, which is dependent on the oxidation states of the elements and may change during calcination of catalyst pretreatment, remains unspecified. The catalyst powders obtained were ground in the GC vial, after which each catalyst powder was weighed and mixed with the appropriate amount of soot (Printex-U). It is well known that Printex-U shows similar properties as diesel soot [20]. An and McGinn have suggested that real soot will combusts at slightly lower temperatures (5–20 °C) than Printex-U [21].

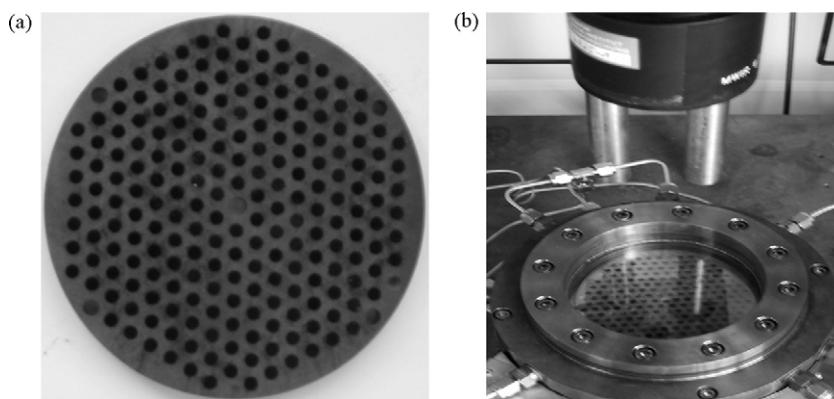


Fig. 1. (a) A slate plate with 206 catalyst–soot samples and (b) IR-camera and reactor with catalyst library for IR-thermography.

The catalyst–soot mixtures (10 mg) were manually transferred into the wells of the slate library plate.

## 2.2. High-throughput experimentation

The purpose of this study is the relative evaluation of catalysts for soot combustion. This is best achieved with a standard model soot of well-defined properties. As model soot the commercial soot Printex-U was chosen, which has a medium particle size of 25 nm and a surface area of  $\sim 100 \text{ m}^2/\text{g}$ . Since soot combustion is an exothermic reaction without additional side or secondary reactions, emissivity-corrected infrared thermography (ec-IRT) for parallel primary screening is principally applicable. However, unlike in gas-phase reactions, where the heat of reaction remains constant under stationary conditions, the heat of reaction, the emissivity and reflectivity of the catalyst–soot spots of soot combustion are time-dependent and change with increasing combustion. This phenomenon makes catalyst evaluation by ec-IRT difficult, since identical reaction conditions are prerequisite to compare catalyst performances on a library.

The catalytic combustion of soot requires interaction of catalyst and soot. This can be achieved by mixing the selected model soot (Printex-U) with the catalyst or by coating the catalyst with a thin layer of soot. The coating of a catalyst library with a soot film is less time-consuming, but prone to errors. Initial attempts to coat a soot layer on a catalyst library with an air brush were successful, but the results obtained were not reproducible. This was attributed to lack of control over the amount and interaction of the soot layer on the different catalysts. Furthermore, ec-IRT screening is only effective, once most of the soot layer has been combusted, so the signal is not only dependent on relative catalytic activity, but also on time and layer thickness of the soot on the catalyst samples. More successful was the method of mixing the catalyst and soot before testing. The catalyst and soot (8 mg and 2 mg, respectively) were combined and mixed loosely with a spatula as explained elsewhere [15]. While the model soot is well defined, the small amount of catalyst produced is first crushed manually before loosely mixed with the soot. Here the method relies on the identical preparation of the catalysts and the use of identical synthesis and calcination procedures. The mixture was

then manually filled into the 206 hexagonally positioned wells in the library plate (see Fig. 1a). The manual filling of the library is also the present bottle neck of this method. The library made of slate was placed in the gas-phase flow reactor shown in Fig. 1b [12]. The reactant gas, which transports heat to or from the reactor is made to enter the reactor on evenly distributed gas-inlet holes above the library around the reactor. The effluent gas leaves the reaction chamber through a central hole on the slate library. This central hole connects to a series of outlet holes below the library slate. These gas-inlet and -outlet arrangement guaranteed an even gas distribution in the reactor. For the feed gas synthetic air was chosen. Although the oxygen content in real motor exhaust is significantly below 10%, in preliminary experiments it was found, that by increasing the oxygen content from 6% to 21% the  $T_{50}$  of soot combustion decreased by 36 °C. Therefore 21% oxygen in nitrogen was chosen for all experiments to ensure high reactivity and compatibility to our thermal analysis equipment. The IR-transparent sapphire window on top of the reactor allows direct recording of temperature changes with the IR-Camera (PtSi-FPA-detector  $648 \times 484$  pixels). Prior to the catalytic reaction, the detector response and the emissivity across the library were corrected by measuring the emissivity of the library at six different temperatures around the desired reaction temperature ( $\pm 5$ ) under a constant flow of nitrogen at 50 ml/min. After calibration, an IR-image of the library recorded at the desired reaction temperature was stored to act as background image for further images under reaction conditions. Synthetic air was then flown through the system (50 ml/min) and the first reaction image was taken after 2 min. After 5 min, 10 min, 15 min, and 20 min, further images were taken, then the gas flow was switched to nitrogen and the last image was stored after additional 5 min. This last image was to document any emissivity changes that might have occurred in the course of the reaction. The library was heated to the next desired temperature and the correction and measurement procedures were repeated (200 °C, 250 °C, 300 °C, 350 °C, and 400 °C). Overall, as indicated already in the text, there are several potential sources for errors and the procedure applied clearly a compromise to allow for rapid screening. Therefore these primary screening data are only used for selection, while conventional testing is crucial to validate the performance of the best catalysts.

### 2.3. Conventional catalyst synthesis and characterization

In order to validate the activities of the best materials from HTE, the samples had to be synthesized conventionally. The preparation of  $\text{Co}_{20}\text{Mo}_{40}\text{Ce}_{40}$ , f.e., was as follows: the complexing agent 4-hydroxyl-4-methyl-2-pentanone (1.86 ml) was pipetted into a 20-ml vial. Subsequently, 1 ml (1 mmol) of a 1-M solution of cobalt nitrate in methanol, 2 ml (2 mmol) of a 1-M solution of molybdenum isopropoxide in 2-propanol and 2 ml (2 mmol) of a 1-M solution of cerium nitrate in methanol were added while stirring. Propionic acid (0.2 mmol, 15  $\mu\text{l}$ ) was added dropwise under continuous stirring. The solution was further stirred for 3 h and then dried at 40 °C until gelation occurred (5 days).

Both thermogravimetric analysis and tubular flow reactors are commonly used in the literature to screen potential soot oxidation catalysts. In this study a Shimadzu TGA-50 was used to validate the potential soot oxidation catalysts identified by the ec-IRT method. Prior to the reaction, a sample of each conventionally prepared catalyst material was heated at a heating rate of 10 °C/min to 700 °C to identify potential material-specific weight changes that may mask the TGA signal resulting from soot oxidation before testing the soot–catalyst mixture. The pre-heating step was particularly important for materials calcined at 400 °C because they may still contain residual organics. However in all tests no significant weight loss was observed. 3 mg of soot was mixed loosely with 12 mg of catalyst in a GC vial before being transferred to the TGA crucible. Maintaining a fixed soot–catalyst ratio is very important to achieve reproducible results. The mixture was heated from 25 °C to 700 °C at a heating rate of 10 °C/min in a 50-ml/min synthetic air flow. The activity of a catalyst was defined by the temperature, where 50% of the soot is oxidised ( $T_{50}$ ). To verify the reproducibility of results, a series of reproduction tests were performed. In these reproduction experiments the  $T_{50}$  has always been reproducible to within 5 °C. The BET surface areas of the lead catalysts were determined by physisorption measurements after calcinations (Sorptomatic 1990, Carlo Erba). X-ray diffraction studies were performed with a Huber G670 Guinier-camera using Cu K $\alpha$  radiation ( $\lambda = 1.54056 \text{ \AA}$ ). Lattice parameter refinement was done by full pattern Rietveld refinement with the program TOPAS [22] using the fundamental parameters approach [23]. A transmission electron microscope from Jeol Corporation of type JEOL JEM-2011 (LaB<sub>6</sub> emitter, 200 kV accelerator voltage) was used to characterise the catalysts. An electron dispersive X-ray (EDX) analyser with SiLi-detector from Oxford Instruments coupled to the transmission electron microscope (TEM) was applied to analyse points on the TEM image.

## 3. Results

### 3.1. High-throughput results

The search strategy considered in this study is based on the concept of evolution, as already applied successfully in earlier

studies [12]. Binary mixed oxides are selected by performance (heat of reaction), compositions of hits are optimized in a follow-up library. Improvement of hits is attempted by doping of the optimized binaries. Again, composition of hits is optimized, followed by another round of doping. This is continued until there is no further improvement. Two strategies can be considered for the choice of elements used in a combinatorial study: (i) the selection could be based on prior information on the activity of the element on a particular reaction (experience), or (ii) elements are chosen randomly with no precedence to catalytic performance [26]. In this study both strategies have been applied. Already in the preceding study, Co-based oxides belonged to the most promising materials identified in a diverse screening study, [15] confirming other studies, which have shown that  $\text{CoO}_x$  is an active catalyst for soot oxidation [6,24,25]. Neeft et al. noticed a strong activity of a  $\text{Co}_3\text{O}_4$  catalyst under tight contact with soot, but the same sample was inactive under loose contact. So  $\text{CoO}_x$  represented the matrix oxide of this study. Library-1 was designed by doping cobalt oxide with 50 different elements at a molar concentration of 3%. Among the catalysts, the best one without alkaline ions or alkaline earth ions was  $\text{La}_3\text{Co}_{97}$ , which rated fifth best. The activity of the alkaline-doped samples has been reported elsewhere [16]. With the emphasis on alkaline-free catalysts, a binary composition spread of the two elements La and Co was prepared and studied, it led to an optimum composition of  $\text{La}_5\text{Co}_{95}$  (results not shown here). The library-2 samples were obtained by doping  $\text{La}_5\text{Co}_{95}$  with 50 different elements at a molar concentration of 3% and 10%. The aim here was to further improve the activity of the  $\text{La}_5\text{Co}_{95}$  catalyst. The IR-images of library-2 at 350 °C and 400 °C are given in Figs. 2 and 3, respectively. At a reaction temperature of 350 °C, only  $\text{Pb}_{10}\text{La}_5\text{Co}_{85}$  was considerably active. When library-2 was tested at 400 °C, two additional samples,  $\text{Na}_{10}\text{La}_5\text{Co}_{85}$  and  $\text{Ce}_{10}\text{La}_5\text{Co}_{85}$ , became active. As expected, the activity of  $\text{Pb}_{10}\text{La}_5\text{Co}_{85}$  decreased because most of the soot had been combusted already at 300 °C. Pb has been known already to improve the activity of soot combustion catalysts [27]. On the other hand, because of its toxicity Pb is not a welcome element in the automobile industry. The primary reason for the improved catalytic activity by lead is believed to be due to the low melting point of lead compounds, which brings about a better contact between catalyst and soot. Nevertheless, this discovery through HT-experimentation is by itself an additional validation of the ec-IRT approach used here.

As already mentioned above, Neeft and Makkee have shown that simple oxides of Ce, Co, La, V, and Mo are active catalyst for soot combustion under tight contact with soot [4]. In our previous study, Ce- and Co-based oxides were most active [15]. In order to determine the best soot oxidation mixed oxide from these elements, a pentanary composition spread of these five elements was designed by varying each elemental molar concentration from 0 to 100 at 20% intervals, whereby 126 samples were synthesized (library-3). Library-3 results are shown in Fig. 4. At 300 °C under synthetic air flow, few catalysts were active in promoting soot combustion, the best catalyst was  $\text{Ce}_{40}\text{Co}_{20}\text{V}_{20}\text{La}_{20}$  followed by  $\text{Ce}_{60}\text{Co}_{20}\text{La}_{20}$  and



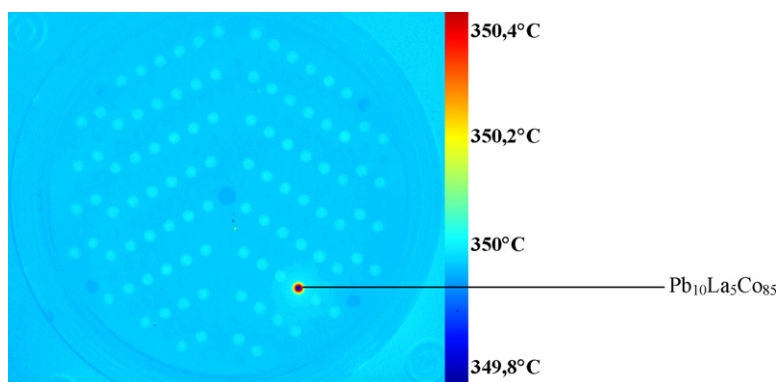


Fig. 2. The emissivity-corrected IR-thermographic image of catalyst library-2 at 350 °C for the combustion of soot.

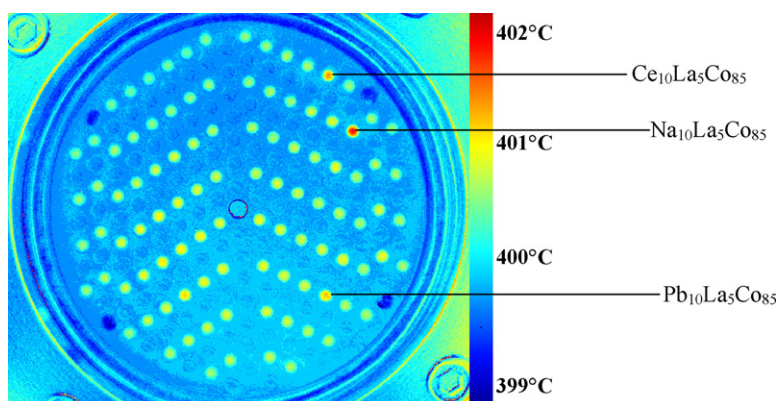


Fig. 3. The emissivity-corrected IR-thermographic image of catalyst library-2 at 400 °C for the combustion of soot.

$\text{Ce}_{60}\text{Co}_{20}\text{Mo}_{20}$ , respectively. The pentanary mixture was inactive for soot combustion. The only binary mixed oxide among the best 10 ranked samples was  $\text{Ce}_{80}\text{La}_{20}$ . Among these mixed oxides  $\text{Ce}_{60}\text{Co}_{20}\text{Mo}_{20}$  showed the highest activity during validation of the performance with TGA (see Table 1, library-3). This promising result motivated us to have a closer look at the relationship between the concentration of each metal oxide in the ternary mixed oxide and the ability of the sample to combust soot. To determine the best composition of the ternary oxide Ce, Co, and Mo, a composition spread library was prepared, whereby each element content was varied from 5% to 100% at 5% interval. From these 236 materials only 195

selected samples (materials low in Ce, rich in Co, Mo, and several binaries were left out) were synthesized and characterised for soot combustion in order to be able to test all the samples in one library (library-4). Fig. 5 shows the IR-image of this ternary composition spread library-4. Among several active samples, the three best samples in this library were  $\text{Ce}_{10}\text{Co}_{65}\text{Mo}_{25}$ ,  $\text{Ce}_{50}\text{Co}_{15}\text{Mo}_{35}$ , and  $\text{Ce}_{60}\text{Co}_{20}\text{Mo}_{20}$ , respectively, therefore only two samples were more active compared to the  $\text{Ce}_{60}\text{Co}_{20}\text{Mo}_{20}$  sample. No clear trend could be noticed with respect to the relationship between the catalyst activity and the concentration of each element. The most significant trend observed here was that all the three oxides are important for the

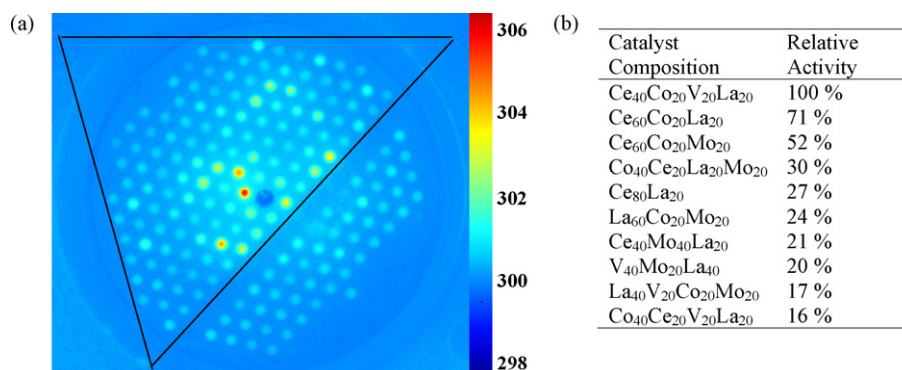


Fig. 4. The emissivity-corrected IR-thermographic image of catalyst library-3 at 300 °C for the combustion of soot. Catalytic composition and relative activity of the selected catalysts on the library.

Table 1  
TGA of selected catalysts for the oxidation of soot with synthetic air

	Catalyst	$T_{50}$ (°C)
Non-catalytic soot oxidation		600
	La <sub>3</sub> Co <sub>97</sub>	547
	La <sub>5</sub> Co <sub>95</sub>	520
Library-2	Pb <sub>10</sub> La <sub>5</sub> Co <sub>85</sub>	433
	Na <sub>10</sub> La <sub>5</sub> Co <sub>85</sub>	490
	Ce <sub>10</sub> La <sub>5</sub> Co <sub>85</sub>	504
Library-3	Ce <sub>60</sub> Co <sub>20</sub> Mo <sub>20</sub>	490
	Ce <sub>60</sub> Co <sub>20</sub> La <sub>20</sub>	514
	Co <sub>40</sub> Mo <sub>20</sub> La <sub>40</sub>	521
	Ce <sub>40</sub> Co <sub>20</sub> V <sub>20</sub> La <sub>20</sub>	528
	Ce <sub>50</sub> Co <sub>15</sub> Mo <sub>35</sub>	451
Library-4	Ce <sub>60</sub> Co <sub>20</sub> Mo <sub>20</sub>	490
	Ce <sub>30</sub> Mo <sub>80</sub>	502
	Ce <sub>25</sub> Mo <sub>60</sub> Mo <sub>15</sub>	511

catalytic activity. Just one binary mixed oxide (Ce<sub>20</sub>Mo<sub>80</sub>) was among the 10 best catalysts in this library. The actual catalytic phase responsible for the activity of the ternary mixed oxides is not clear at this stage.

### 3.2. Conventional test results

In order to validate the soot oxidation activities of the best catalysts discovered through the high-throughput experimentation technique, the temperature-dependent soot weight change was determined by thermogravimetric analysis. Fig. 6 shows the TGA curves for soot combustion by La<sub>3</sub>Co<sub>97</sub> and La<sub>5</sub>Co<sub>95</sub>. It can be clearly seen from these curves that the activity of the La<sub>5</sub>Co<sub>95</sub> catalyst is higher than that of La<sub>3</sub>Co<sub>97</sub>. When mixed with soot, La<sub>5</sub>Co<sub>95</sub> combusted 50% of soot at 520 °C ( $T_{50}$ ) while La<sub>3</sub>Co<sub>97</sub> combusted 50% of soot at 547 °C. The  $T_{50}$  values of the most active catalysts of library-2 (M<sub>x</sub>La<sub>5</sub>Co<sub>95-x</sub>) are given in Table 1. Here the Pb<sub>10</sub>La<sub>5</sub>Co<sub>85</sub> sample was most active with a  $T_{50}$  of 433 °C (confirming the HTE), followed by Na<sub>10</sub>La<sub>5</sub>Co<sub>85</sub> with a  $T_{50}$  of 490 °C. The addition of Pb, Na, or Ce as a third element to the binary mixed oxide lead to an improved catalytic activity. It should be mentioned that the  $T_{50}$  value for the non-catalysed soot combustion is around 600 °C.

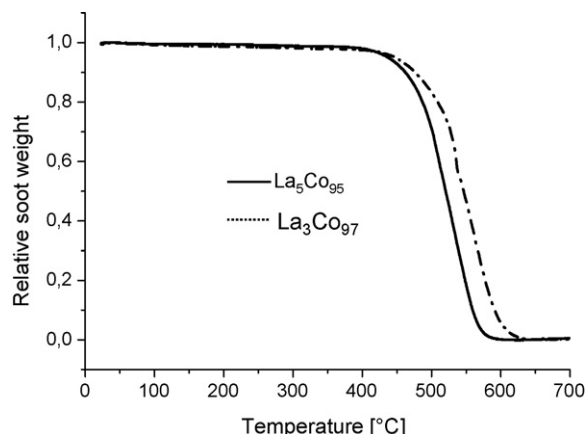


Fig. 6. Comparison of TGA curves for soot oxidation by La<sub>3</sub>Co<sub>97</sub> and La<sub>5</sub>Co<sub>95</sub> catalysts.

Relative to the undoped La<sub>5</sub>Co<sub>95</sub> the  $T_{50}$  value decreased by 87 °C for Pb<sub>10</sub>La<sub>5</sub>Co<sub>85</sub>. This result agrees with the literature [27], although comparison with other studies should be made with caution because of the specificities of the reaction conditions, such as soot–catalyst contact type, heating rate, etc. A good correlation was observed between the HTE results and the TGA results for the M<sub>x</sub>La<sub>5</sub>Co<sub>95-x</sub> library samples.

To determine the effect of the calcination temperature on the activity of the Pb<sub>10</sub>La<sub>5</sub>Co<sub>85</sub> sample, four different Pb<sub>10</sub>La<sub>5</sub>Co<sub>85</sub> samples were synthesized and calcined at 400 °C, 500 °C, 600 °C, and 700 °C in air for 5 h. The calcined samples were mixed with soot and submitted to TGA with a temperature range from 25 °C to 700 °C under a flow of synthetic air. The soot combustion temperature  $T_{50}$  as a function of the calcination temperature is given in Fig. 7. It was surprising to note that there is little effect of calcination temperature on the activity of the catalyst. The variations observed may not be significant and the good activity observed for the sample treated at 700 °C is indicative of a high temperature stability of these catalysts. Another indication for the high stability of this Pb-containing catalyst has been obtained by repeated soot-oxidation experiments, where the used catalyst was mixed three times with fresh soot and

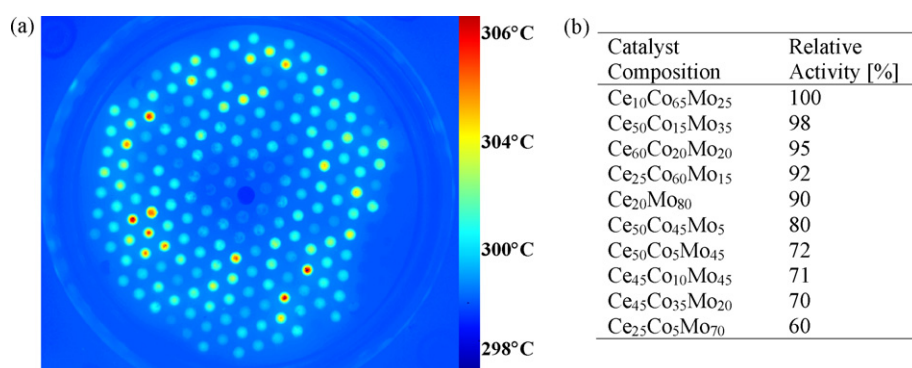


Fig. 5. (a) The emissivity-corrected IR-thermographic image of catalyst library-4 at 300 °C for the combustion of soot. (b) Catalytic composition and relative activity of the selected catalysts on the library.

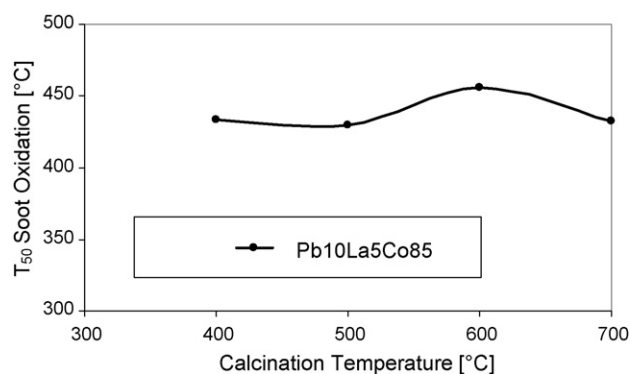


Fig. 7. The temperature at which 50% of soot is combusted ( $T_{50}$ ) as a function of the calcination temperature.

subjected to the TGA test. All TGA data were identical, indicating an excellent stability.

The TGA results of the pentanary composition spread library-3 (Table 1) give the best  $T_{50}$  value of 490 °C for the  $\text{Ce}_{60}\text{Co}_{20}\text{Mo}_{20}$  catalyst. None of the other catalysts on this library had a  $T_{50}$  value below 500 °C. Even the best catalyst from HTE,  $\text{Ce}_{40}\text{Co}_{20}\text{V}_{20}\text{La}_{20}$ , showed only a  $T_{50}$  value of 528 °C. This discrepancy between the HTE data and the TGA results was to be expected and can be attributed to the differences between the measurements (single image during combustion by ec-IRT and integral analysis of the complete soot combustion by TGA). Due to not comparable reaction conditions of ec-IRT and TGA, the light off temperatures observed cannot be compared directly. In the ec-IRT experiments we search for the most active material at the lowest temperature possible. Therefore, also the relative ranking in the two methods may not correspond precisely. Nevertheless, the catalysts which were active during the HT experiments also showed activity during TGA experimentation which was more important in this study than the ranking. For evaluation the relatively low temperatures observed by ec-IRT are only considered as a screening result, for practical evaluation, only the TGA data should be chosen.

To confirm the activity of the library-4 hits discovered via IR-thermography, additional TG analyses were performed. As shown in Table 1,  $\text{Ce}_{50}\text{Co}_{15}\text{Mo}_{35}$  with a  $T_{50}$  at 451 °C was more active compared to  $\text{Ce}_{60}\text{Co}_{20}\text{Mo}_{20}$ . No trend could be noticed with respect to the relationship between catalyst activity and the elemental concentration. Significant is the high concentration of ceria, a well known oxide for soot combustion whose activity is attributed to its oxygen storage and release potential.  $\text{CeO}_2$  itself, when prepared by the same sol–gel procedure, has a  $T_{50}$  of 495 °C, so addition of Mo and Co to the mixed oxide reduced the  $T_{50}$  of soot oxidation by >40 °C.  $\text{Ce}_{50}\text{Co}_{15}\text{Mo}_{35}$  is therefore the other promising new mixed oxide, discovered in this HT-investigation. Another noble metal-free reference material studied here, Cs–Fe–V/ $\text{Al}_2\text{O}_3$ , showed a  $T_{50}$  of 493 °C. It has been reported to show an ignition temperature of 322 °C, obtained however under different conditions and with tight contact between soot and catalysts [28].

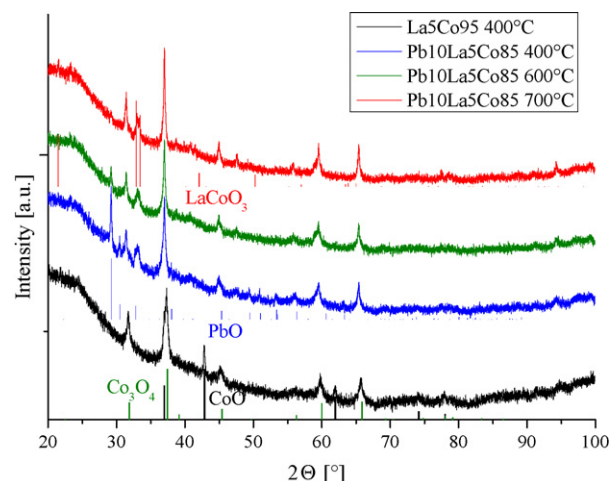


Fig. 8. Powder XRD patterns of  $\text{La}_5\text{Co}_{95}$  calcined at 400 °C,  $\text{Pb}_{10}\text{La}_5\text{Co}_{85}$  calcined at 400 °C, 600 °C, and 700 °C (from bottom up) with JCPDS data (CoO: 78-431;  $\text{Co}_3\text{O}_4$ : 71-816; PbO: 72-93;  $\text{LaCoO}_3$ : 84-846).

### 3.3. Characterization results

The catalysts  $\text{La}_5\text{Co}_{95}$  and  $\text{Pb}_{10}\text{La}_5\text{Co}_{85}$  were identified as potential soot oxidation catalyst. In order to identify the phases present in these samples, XRD measurements were conducted and the obtained XRD patterns are depicted in Fig. 8. In the binary mixed La–Co oxide sample, whose diffraction pattern is shown at the bottom, only the phases  $\text{Co}_3\text{O}_4$  and CoO (JCPDS—CoO: 78-431;  $\text{Co}_3\text{O}_4$ : 71-816) could be identified. The element La as dopant on the Co positions is distributed statistically over these lattice positions and thus not resulting in additional diffraction peaks. From bottom up, the next diffractogram denotes the pattern of the  $\text{Pb}_{10}\text{La}_5\text{Co}_{85}$  sample which was calcined at 400 °C. The phases  $\text{Co}_3\text{O}_4$ ,  $\text{LaCoO}_3$  (hexagonal perovskite) and PbO (massicot) (JCPDS— $\text{LaCoO}_3$ : 84-846; PbO: 72-93) could be identified and were present with small particles sizes, but not any longer CoO. Table 2 gives the phase fractions as result from Rietveld refinements with the program TOPAS. The crystallinity of this sample was very poor, which may be attributed to the third element added and a highly amorphous nature of the sample. The improved reducibility of the mixed valent  $\text{Co}_3\text{O}_4$  to CoO may be responsible for the observed catalytic activity of these samples. The relatively weak bond strength of the Co–O bond in  $\text{Co}_3\text{O}_4$  increases the availability of lattice oxygen. It seems logical to attribute the superior soot combustion activity of these catalysts to the presence of  $\text{Co}_3\text{O}_4$ , however, solely on that basis this cannot explain the higher catalytic activity of the Pb-doped samples, because the phase fraction of  $\text{Co}_3\text{O}_4$  is almost the same in all investigated samples, as shown in Table 2. The reducibility of the  $\text{Co}_3\text{O}_4$  crystallites is known to be enhanced by the presence of other phases such as the CuO phase, because Cu is also observed in oxidation state +1. Here the presence of CoO in  $\text{La}_5\text{Co}_{95}$  might have just the reverse effect, a reduction of reducibility of  $\text{Co}_3\text{O}_4$ , because  $\text{Co}^{2+}$  is at least the lowest possible oxidation state for Co. Additionally or alternatively, the additional phase  $\text{LaCoO}_{3-\delta}$  present in  $\text{Pb}_{10}\text{La}_5\text{Co}_{85}$  samples

Table 2

Phase fractions from powder XRD data by Rietveld refinement with TOPAS

Sample	$x(\text{Co}_3\text{O}_4)$	$x(\text{CoO})$	$x(\text{LaCoO}_3)$	$x(\text{PbO})$
$\text{La}_5\text{Co}_{95}$ 400 °C	0.876	0.124	–	–
$\text{Pb}_{10}\text{La}_5\text{Co}_{85}$ 400 °C	0.848	–	0.097	0.055
$\text{Pb}_{10}\text{La}_5\text{Co}_{85}$ 600 °C	0.878	–	0.106	0.016
$\text{Pb}_{10}\text{La}_5\text{Co}_{85}$ 700 °C	0.874	–	0.123	0.002

Table 3

Lattice parameters of  $\text{Co}_3\text{O}_4$  and  $\text{La}_{1-x}\text{Pb}_x\text{CoO}_{3-\delta}$  by Rietveld refinement with TOPAS

Sample	$\text{Co}_3\text{O}_4$	$\text{La}_{1-x}\text{Pb}_x\text{CoO}_{3-\delta}$	
	$a$ (Å)	$a$ (Å)	$c$ (Å)
$\text{La}_5\text{Co}_{95}$ 400 °C	8.081(1)	–	–
$\text{Pb}_{10}\text{La}_5\text{Co}_{85}$ 400 °C	8.086(1)	5.438(1)	13.24(1)
$\text{Pb}_{10}\text{La}_5\text{Co}_{85}$ 600 °C	8.088(1)	5.447(1)	13.184(5)
$\text{Pb}_{10}\text{La}_5\text{Co}_{85}$ 700 °C	8.087(1)	5.448(1)	13.136(2)

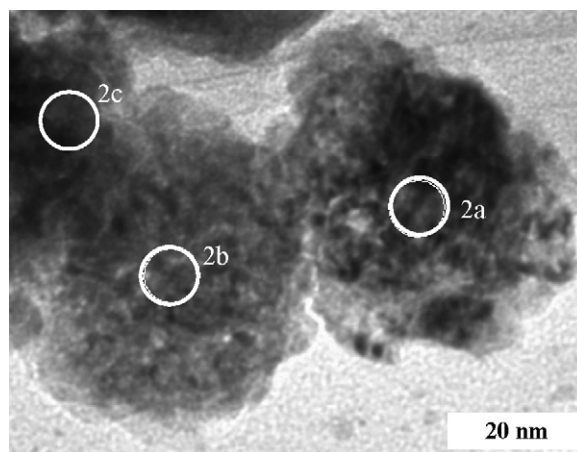
is reported to have oxygen vacancies in the anionic sublattice. This means that the Co in this compound is also mixed valent, which can be expressed by the formula  $\text{LaCo}^{3+}_{1-x}\text{Co}^{2+}_x\text{O}_{3-x/2}$ . The larger  $\text{Co}^{2+}$  cation is expanding the lattice, so that even if the oxygen content is reduced with increasing  $\text{Co}^{2+}$  fraction the lattice parameter  $c$  of the hexagonal unit cell increases with  $x$  [28]. Probably the addition of  $\text{PbO}$  in  $\text{LaCoO}_{3-\delta}$  resulted in a stabilization of the latter phase and thus in an enhanced reducibility of  $\text{CoO}_x$  towards soot combustion. Also examined was the effect of the calcination temperature on the phase composition and crystallinity of the  $\text{Pb}_{10}\text{La}_5\text{Co}_{85}$  catalyst. All the samples irrespective of the calcination temperature showed the same amount of the  $\text{Co}_3\text{O}_4$  phase (see Tables 2 and 3). At 400 °C also  $\text{PbO}$  was observed, which disappeared at higher temperatures up to 700 °C accompanied by lattice parameter shift of the neighbouring phase  $\text{LaCoO}_{3-\delta}$ , which is detectable apart from  $\text{Co}_3\text{O}_4$  in all  $\text{Pb}_{10}\text{La}_5\text{Co}_{85}$  samples. Clearly, the crystallinity of the sample was also increasing with increasing calcination temperature. But the loss of activity due to sintering and surface area reduction is compensated by an increased reducibility of the compound  $\text{Pb}^{2+}_y\text{La}^{3+}_{1-y}\text{Co}^{3+}_{1-x+y}\text{Co}^{2+}_{x-y}\text{O}_{3-x/2}$  at higher calcination temperatures when  $x$  decreases and  $y$  increases. That  $x$  decreases can be seen from Table 3, in which the  $c$  lattice parameters of  $\text{LaCoO}_{3-\delta}$  decrease with calcination temperature. On the other side the incorporation of the element Pb into the  $\text{LaCoO}_{3-\delta}$  lattice increases its thermal stability and thus reduces its volatility.

The XRD results were complemented by transmission electron microscopy studies. The TEM was equipped with EDX. For each catalyst, a good correlation between the

Table 4

Results of the EDX analyses of  $\text{Pb}_{10}\text{La}_5\text{Co}_{85}$  catalyst at specific points

Position	Co–K (at.%)	La–L (at.%)	Pb–L (at.%)
2a	88.04	4.44	7.53
2b	91.4	4.5	4.09
2c	84.3	4.68	11.02

Fig. 9. TEM image of the  $\text{Pb}_{10}\text{La}_5\text{Co}_{85}$  catalyst with markings indicating EDX analyses points.

expected elemental distribution and the observed elemental distribution was achieved. A representative micrograph of the  $\text{Pb}_{10}\text{La}_5\text{Co}_{85}$  catalyst is given in Fig. 9. A relatively homogeneous elemental distribution was achieved by spot analysis with 20-nm diameter and larger (Table 4). This observation suggested a homogeneous distribution of the various constituents of the catalyst. No indication of domain formation was obtained, except for the phases identified by XRD. The BET measurements revealed that the doping of the  $\text{LaCo}$  sample with Pb led to a decrease in the sample surface area. The specific surface area of  $\text{La}_5\text{Co}_{95}$  was  $47.2 \text{ m}^2/\text{g}$  while that of  $\text{Pb}_{10}\text{La}_5\text{Co}_{85}$  was  $24.5 \text{ m}^2/\text{g}$ . This finding suggests that a factor different from simple surface area effects must be responsible for the improved catalytic activity observed after doping with lead (see above).

#### 4. Conclusion

A combinatorial method for the development of mixed metal oxide catalysts for soot combustion has been applied successfully to search for new catalysts. The binary mixed oxide  $\text{La}_5\text{Co}_{95}$  was found to possess significant activity for soot combustion. The doping of this binary catalyst with 50 different metal oxides resulted in the more active material  $\text{Pb}_{10}\text{La}_5\text{Co}_{85}$ . Though the presence of lead in this sample put to question its possible application in real diesel exhaust systems, this discovery was important considering the low soot combustion temperature achieved with this catalyst. Investigations of the influence of the calcination temperatures on this catalysts showed that the catalyst activity is almost constant when calcined between 400 °C and 700 °C indicating a high thermal stability of the material, which was confirmed by the discovery of the new lead–cobalt–oxide phases formed upon the high temperature treatment. A ternary composition spread of the metal oxides of Ce, Co, and Mo provided  $\text{Ce}_{50}\text{Co}_{15}\text{Mo}_{35}$  with a soot oxidation temperature 150 °C lower than that of uncatalysed soot oxidation, a new material of promising oxidation activity and acceptable composition. The study has shown that good soot oxidation catalysts free of noble metal



and alkaline metals exist and can be found readily with the use of suitable high-throughput technologies.

### Acknowledgements

The authors thank J. Jockel and C. Pokorna for discussions, J. Schmauch for the TEM studies and Robert Bosch GmbH for support.

### References

- [1] J.-M. Seo, H.-S. Chang, S.-K. Kim, SAE Paper 2006-01-0422, 2006.
- [2] S.G. Nickolas, A.D. White, A.J. Kotrba, A. Yetkin, SAE Paper 2006-01-1089, 2006.
- [3] G. Mul, F. Kapteijn, C. Doornkamp, J.A. Muolijin, *J. Catal.* 179 (1998) 258.
- [4] J.P.A. Neeft, M. Makkee, J.A. Muolijin, *Appl. Catal. B* 8 (1996) 57.
- [5] B.A.A.L. van Setten, J.M. Schouten, M. Makkee, J.A. Moulijn, *Appl. Catal. B* 28 (2000) 253.
- [6] J.P.A. Neeft, M. Makkee, J.A. Moulijn, *Fuel* 77 (3) (1998) 111.
- [7] R. Vijay, C.M. Snively, J. Lauterbach, *J. Catal.* 243 (2006) 368.
- [8] G. Grubert, S. Kolf, M. Baerns, A.C. van Veen, C. Mirodatos, E.R. Stobbe, P.D. Cobden, *Appl. Catal. A* 306 (2006) 17.
- [9] Y. Yamada, T. Kobayashi, *J. Jpn. Petrol. Inst.* 49 (2006) 157.
- [10] S. Hannemann, J. Grunwaldt, P. Lienemann, D. Günther, F. Krumeich, S.E. Pratsinis, A. Baiker, *Appl. Catal. A* 316 (2007) 226.
- [11] D.-K. Kim, W.F. Maier, *J. Catal.* 238 (2006) 142.
- [12] J. Saalfrank, W.F. Maier, *Angew. Chem. Ed.* 43 (2004) 2028.
- [13] G. Kirsten, W.F. Maier, *Appl. Surf. Sci.* 223 (2004) 87.
- [14] H. An, C. Kilroy, P.J. McGinn, *Catal. Today* 98 (2004) 423.
- [15] N.E. Olong, K. Stöwe, W.F. Maier, *Appl. Catal. B* 74 (2007) 19.
- [16] C.A. Querini, L.M. Cornaglia, M.A. Ulla, E.E. Miro, *Appl. Catal.* 20 (1999) 165.
- [17] G. Frenzer, W.F. Maier, *Annu. Rev. Mater. Res.* 36 (2006) 281.
- [18] J. Klein, W.F. Maier, *Chem. Mater.* 11 (1999) 2584.
- [19] J. Scheidman, J. Saarfrank, W.F. Maier, *Stud. Surf. Sci. Catal.* 145 (2003) 13.
- [20] J.P.A. Neeft, M. Makkee, J.A. Moulijn, *Fuel* 76 (12) (1997) 1129.
- [21] H. An, P.J. McGinn, *Appl. Catal. B* 62 (2006) 46.
- [22] TOPAS, version 2.1, Bruker AXS, Karlsruhe, 2003.
- [23] R.W. Cheary, A.A. Coelho, *J. Appl. Cryst.* 25 (1992) 109.
- [24] P.G. Harrison, I.K. Ball, W. Daniell, P. Lukinskas, M. Cespedes, E.E. Miro, M.A. Ulla, *Chem. Eng. J.* 95 (2003) 47.
- [25] V.E. Genc, F.E. Altay, D. Uner, *Catal. Today* 105 (2005) 537.
- [26] C. Klanner, D. Farrusseng, L. Baumes, C. Mirodatos, F. Schüth, *QSAR Comb. Sci.* 22 (2003) 729.
- [27] D. Uner, M.K. Demirkol, B. Dernaika, *Appl. Catal. B* 61 (2005) 334.
- [28] G. Neri, G. Rizzo, S. Galvagno, A. Donato, M.G. Musolino, R. Pietro-paolo, *Appl. Catal. B* 42 (2003) 381.